

Photodisintegration of Three-Body Nuclei with Realistic 2N and 3N Forces

Victor D. Efros¹, Winfried Leidemann², Giuseppina Orlandini² and Edward L. Tomusiak³

¹*Russian Research Centre "Kurchatov Institute", Kurchatov Square, 1, 123182 Moscow, Russia*

²*Dipartimento di Fisica, Università di Trento, and*

Istituto Nazionale di Fisica Nucleare, Gruppo collegato di Trento, I-38050 Povo, Italy

³*Department of Physics and Engineering Physics*

University of Saskatchewan, Saskatoon, Canada S7N 0W0

(October 17, 2018)

Abstract

Total photonuclear absorption cross sections of ^3H and ^3He are studied using realistic NN and NNN forces. Final state interactions are fully included. Two NN potential models, the AV14 and the r-space Bonn-A potentials, are considered. For the NNN forces the Urbana-VIII and Tucson-Melbourne models are employed. We find the cross section to be sensitive to nuclear dynamics. Of particular interest in this work is the effect which NNN forces have on the cross section. The addition of NNN forces not only lowers the peak height but increases the cross section beyond 70 MeV by roughly 15%. Cross sections are computed using the Lorentz integral transform method.

arXiv:nucl-th/9911049v2 3 Mar 2000

The process of nuclear photoabsorption is known to be strongly dependent on exchange currents and hence on the underlying nuclear dynamics. One therefore expects the photoabsorption cross section to be sensitive to NN and NNN nuclear forces. It is the purpose of this paper to explore this sensitivity by computing the total photoabsorption cross sections of the trinucleons by using realistic NN and NNN potentials. The only other calculations of trinucleon photodisintegration covering a larger range of energies (0 - 40 MeV) and employing realistic NN forces are, to our knowledge, those of Sandhas *et al* [1]. However their calculations are for the exclusive process of two-body breakup while we compute the inclusive (two-body + three-body breakup) cross sections over a larger energy range. It is because we are looking for effects of NN and NNN forces that energies in the tail region, $E_\gamma > 70$ MeV, are included here.

We use the Argonne AV14 potential [2] and the Bonn-A r-space potential [3]. As NNN potentials we include the Urbana-VIII (UrbVIII) [4] and Tucson-Melbourne (TM) [5] NNN models. The total photoabsorption cross section for energies below pion threshold is computed by using the unretarded dipole operator

$$\vec{D} = \sum_{i=1}^Z (\vec{r}_i - \vec{R}_{cm}) . \quad (1)$$

This form of the operator already includes the effects of exchange currents due to Siegert's theorem. It is known that as far as the total cross section is concerned corrections to the unretarded dipole operator are small in the energy range studied here. We consider this approximation adequate for investigating the effects of NN and NNN forces to the process. The total photoabsorption cross section is then given in terms of the dipole response function R by

$$\sigma_{tot} = 4\pi^2 (e^2/\hbar c) E_\gamma R(E_\gamma) \quad (2)$$

where

$$R(\omega) = \langle \Psi_0 | D_z \delta(H - E_0 - \omega) D_z | \Psi_0 \rangle . \quad (3)$$

To calculate $R(\omega)$ we use the Lorentz integral transform method introduced in [6]. This technique eliminates the need to compute final-state continuum wave functions. The transform, $\Phi(\sigma_R, \sigma_I)$, of $R(\omega)$ is defined by

$$\Phi(\sigma_R, \sigma_I) = \int_{\omega_{min}}^{\infty} d\omega \frac{R(\omega)}{(\omega - \sigma_R)^2 + \sigma_I^2} . \quad (4)$$

It can be expressed as the norm of the square integrable function $\tilde{\Psi}$

$$\Phi(\sigma_R, \sigma_I) = \langle \tilde{\Psi} | \tilde{\Psi} \rangle \quad (5)$$

where

$$(H - E_0 - \sigma_R + i\sigma_I) |\tilde{\Psi}\rangle = D_z |\Psi_0\rangle . \quad (6)$$

Finally $R(\omega)$ is obtained by inverting the transform (4). The inversion procedure is elaborated upon in [6,8,7]. This method was applied to the study of few-nucleon responses in

[8–12]. In [9] Faddeev techniques were applied to solve equations of the form of Eq.(6) whereas [8,10–12] used expansions in a set of correlated hyperspherical harmonics (CHH) for this purpose. The latter technique is also adopted in the present work. We expand the functions, Ψ_0 and $\tilde{\Psi}$, in a set of correlated hyperspherical harmonics (CHH) according to

$$\Psi = \tilde{\omega} \sum c_i \phi_i \quad (7)$$

where $\tilde{\omega}$ is a correlation operator and ϕ_i are a totally antisymmetric basis set constructed from a spatial part $\chi_{i,\mu}$ and a spin-isospin part θ_μ

$$\phi_i = \sum_{\mu} \chi_{i,\mu} \theta_{\mu} . \quad (8)$$

Whereas in [8,10,11], where simpler potential models were employed, it was sufficient to take $\tilde{\omega}$ in the state independent form

$$\tilde{\omega} = \prod_{i<j} f(r_{ij}) . \quad (9)$$

we now use a state dependent correlation operator of the form

$$\tilde{\omega} = \mathcal{S} \prod_{i<j} \sum_{S,T} f_{ST}(r_{ij}) \tilde{P}_{ST}(ij) \quad (10)$$

where $P_{ST}(ij)$ are projection operators onto nucleon pairs (ij) with spin S and isospin T and where \mathcal{S} is a particle symmetrization operator. This form of correlation operator is easily incorporated into the calculations by first constructing the set of coefficients $\langle \theta_{\mu'} | \tilde{\omega} | \theta_{\mu} \rangle$ and then writing

$$\Psi = \sum_i \tilde{\chi}_{i,\mu'} \theta_{\mu'} \quad (11)$$

where

$$\tilde{\chi}_{i,\mu'} = \sum_{\mu} \langle \theta_{\mu'} | \tilde{\omega} | \theta_{\mu} \rangle \chi_{i,\mu} . \quad (12)$$

The correlation functions $f_{ST}(r)$ are chosen as follows. For $r < r_0$, the healing distance, $f_{ST}(r)$ is chosen to be the zero energy pair wave function in the corresponding ST state. Healing is insured by imposing the conditions $f_{ST}(r)=1$ for $r > r_0$ and $f'_{ST}(r_0)=0$. The $ST=13$ and 31 cases are determined from the 1S_0 and 3S_1 partial waves of the NN potential. However for the $ST=11$ and 33 cases the 1P_1 and 3P_1 potentials are not sufficiently attractive to obtain a healing distance. Therefore we introduce an additional intermediate range central interaction such that a healing distance of 10 fm is obtained. Further details can be found in [12].

Table 1 gives our results for the ground state properties of ^3H using the various potential models described above. We point out that our results for both the ground state and the Lorentz integral transform arise from fully converged expansions in the CHH basis. The inversion leads to stable results for $R(\omega)$. In order to obtain the correct binding energy with the TM NNN potential we have adjusted the cut-off mass Λ in the monopole form

factor. This requires $\Lambda = 4.67\mu$ and $\Lambda = 4.07\mu$ for use with the AV14 and Bonn-A (r-space) cases respectively. Previously published ground state properties are available [13,14] for the AV14 and AV14+UrbVIII potentials. The corresponding results in Table 1 are in agreement with these. Since the method of the Lorentz integral transform allows one to calculate the cross section over the entire energy range, sum rules can be used to give additional checks. An example is provided by explicit evaluation of the inverse energy weighted sum rule $\sigma_{-1} = \int_{E_{th}}^{\infty} E_{\gamma}^{-1} \sigma_{tot}(E_{\gamma}) dE_{\gamma}$ which is related to the triton point proton radius through

$$\sigma_{-1}(^3\text{H}) = \frac{4\pi^2 e^2}{3 \hbar c} \langle r_p^2(^3\text{H}) \rangle .$$

This sum rule is calculated in two ways: (i) by direct integration of the response giving σ_{-1}^{int} , and (ii) by use of the ground state wave function giving σ_{-1}^{gs} . As seen in Table 1 agreement is obtained to better than 0.5%. This level of agreement helps confirm that the lower energy regions, and especially the peak heights, are correct. A check on the higher energy regions is provided by evaluating the TRK sum rule, again by direct integration and by the ground state expectation value of the appropriate double commutator. This was done for the AV14 model, yielding 70.7 MeV-mb by direct integration and 71.6 MeV-mb by evaluating the double commutator. The direct integration was carried out to 2000 MeV. It should be noted that integrating up to 300 MeV excitation only exhausts about 90% of the sum rule. This is in contrast to the integration of the TRK sum rule produced by a soft-core potential such as TRSB potential [15] where almost all the strength is exhausted at 300 MeV excitation [8].

The value of the cross section at the peak depends on ground state details, especially the radius. This is evident from the remarks above on the inverse energy weighted sum rule. Fig.1, for example, shows results obtained previously [10] using the Malfliet-Tjon (MT) [16] and Trento (TN) [8] potentials together with new results obtained here for the AV14 and AV14+UrbVIII potentials. Ground state point proton radii computed from these potentials are 1.61, 1.59, 1.66, and 1.60 fm respectively. The similar peak heights for these rather different potentials is due largely to the similarity of these radii. However, we have observed that in all cases considered here the combination of realistic NN forces with NNN forces leads to roughly a 10 % decrease in the peak height. Moreover, even though the four potentials give similar radii and binding energies the AV14 and AV14+UrbVIII potentials produce cross sections with significantly larger high energy tails than the semi-realistic MT and TN models. Part of the difference must be attributable to the tensor force contained in the realistic potential models.

Figs.2(a) and 2(b) show the peak and tail regions of the T=1/2 contribution to the absorption cross section as computed from the five potential models of Table 1. A study of these figures reveals that the addition of three-body forces (3BF) lowers the peak height and increases the cross section in the tail region by 10 - 20%. The lowering of the peak can be understood since the addition of 3BF increases the binding energy and decreases the radius in all cases. Despite the increase of the cross section in the tail region due to 3BF, no clear separation between the cross section with and without 3BF is seen in this channel. We note the importance of binding in this T=1/2 channel by observing in the tail region the rather disparate curves for the pure NN cases of AV14 and Bonn-A. Recall from Table 1 that these NN potentials correspond to ^3H binding energies of 7.69 MeV and 8.15 MeV respectively. In

addition the three curves corresponding to the addition of NNN forces are rather close and difficult to distinguish, reinforcing the argument that effects here are mainly due to binding.

Curves corresponding to Fig.2 but for the $T=3/2$ channel are shown in Figs.3(a) and 3(b). The behaviour of the cross section in the peak region is similar to the $T=1/2$ case although here the peak height is less sensitive to the interaction model. Fig.3(b) shows that the $T=3/2$ channel clearly separates all models containing a 3BF from those with purely NN forces. This is a 5 - 10 % effect in the energy range 70-110 MeV. However contrary to the $T=1/2$ case, binding effects here do not play an important role as evidenced by the nearly overlapping NN curves in the tail region. As a result the separation between the curves in Fig.3(b) is dominantly an effect due to NNN forces i.e. the $T=3/2$ channel is more sensitive to NNN forces in the tail region. The import of this observation is that it is the three-body breakup channels which might show more evidence of 3BF since they carry all of the $T=3/2$ strength. In fact analyzing our theoretical results and the experimental nd and ppn data from Ref. [18] leads us to conclude that in this energy region the $T=1/2$ content of the ppn channel is about 1/3. Our findings are in line with proposals [17] which suggest particular kinematical set-ups in the nnp or npp channels to be sensitive to the presence of 3BF.

Figs.4(a) and 4(b) compare to available data [18,19] the total cross sections for ${}^3\text{H}$ and ${}^3\text{He}$ as computed with two of our more complete potential models, AV14+UrbVIII and Bonn-A + TM. The ${}^3\text{He}$ calculations include the full Coulomb interaction between the protons. Our calculations agree rather closely with the available data. We note by reference to Fig. 1 that the semi-realistic models do not yield the same level of agreement with the data.

We have computed the total photo-absorption cross sections of the trinucleons by using realistic NN and NNN forces. Final state interactions have been fully included through the use of the Lorentz integral transform method. The results show clear sensitivity to the underlying nuclear dynamics. In particular the tail region of the $T=3/2$ channel appears to be more sensitive to details of the NNN forces than to NN forces. Therefore further theoretical and experimental effort should be devoted to this promising kinematical region. On the theoretical side several corrections, expected to be minor, will be investigated in the future. These are the effects of higher multipoles, retardation in the one-body operators and inclusion of explicit two-body currents beyond the Siegert theorem. In addition the calculation will be extended to the new charge dependent potentials such as the AV18 [20] and Nijmegen [21] potentials together with corresponding NNN models. The rather large effect of the NNN force in the tail region could imply a much larger effect in some selected kinematics of the exclusive three-body breakup reaction. In this regard it should be pointed out that a modification of the Lorentz integral transform method used here [22,23] will allow the calculation of exclusive reaction cross sections as well.

TABLES

TABLE I. ${}^3\text{H}$ Ground state properties for AV14, Bonn-A, AV14+UrbVIII, AV14+TM, and Bonn-A+TM potential models.

Potential	E_B (MeV)	$\sqrt{\langle r_p^2 \rangle}$ (fm)	P_D	σ_{-1}^{int} (mb)	σ_{-1}^{gs} (mb)
AV14	7.69	1.66	8.94	2.636	2.645
Bonn-A	8.15	1.61	6.88	2.481	2.486
AV14+UrbVIII	8.49	1.60	9.67	2.442	2.453
AV14+TM	8.48	1.60	9.67	2.448	2.459
Bonn-A +TM	8.47	1.59	7.25	2.411	2.415

FIGURES

FIG. 1. Total ^3H photoabsorption cross sections predicted by the TN (dotted curve), MT (dashed curve), AV14 (dash-dot curve) and the AV14 + UrbVIII (solid curve) potential models.

FIG. 2. $T=1/2$ part of the ^3H total photoabsorption cross sections in the peak region (a) and tail region (b). The corresponding potentials are AV14 (dotted), AV14 + UrbVIII (short dash), AV14 + TM (long dash), r-space Bonn-A (dash-dot), r-space Bonn-A + TM (solid).

FIG. 3. As in Fig. 2 but for $T=3/2$.

FIG. 4. Total photoabsorption cross sections for ^3H (a) and ^3He (b) computed from the AV14 + UrbVIII (solid) and r-space Bonn-A + TM (dashed) models. The shaded area represents the data from [19] while the black dots are the data of [18].

ACKNOWLEDGMENT

The work of WL, GO, and ELT is partially supported by a NATO Collaborative Research Grant. All authors acknowledge support from the Italian Ministry of Research (MURST). In addition the work of ELT is supported by the INFN and the National Science and Engineering Research Council of Canada.

REFERENCES

- [1] W. Schadow and W. Sandhas, Phys. Rev. **C55**, (1997) 1074; W. Sandhas, W. Schadow, G. Ellerkmann, L.L. Howell and S.A. Sofianos, Nucl. Phys. **A631**, (1998) 210c ; W. Schadow and W. Sandhas, Nucl. Phys. **A631**, (1998) 588c
- [2] R.B. Wiringa, R.A. Smith, and T.L. Ainsworth, Phys. Rev. **C29**, (1984) 1207
- [3] R. Machleidt, Adv. Nucl. Phys. **19**, (1989) 189
- [4] R.B. Wiringa, Phys. Rev. **C43**, (1991) 1585
- [5] S.A. Coon, M.D. Scadron, P.C. McNamee, B.R. Barrett, D.W.E. Blatt and B.H.J. McKellar, Nucl. Phys. **A317**, (1979) 242 ; S.A. Coon and W. Glöckle, Phys. Rev. **C23**, (1981) 1790; S.A. Coon (private communication) giving the most recent parameters as $a' = -1.35\mu^{-1}$, $b = -2.86\mu^{-3}$ and $d = -0.64\mu^{-3}$.
- [6] V.D. Efros, W. Leidemann and G. Orlandini, Phys. Lett. **B338**, (1994) 130
- [7] V.D. Efros, W. Leidemann, and G. Orlandini, Nucl. Phys. **A631**, (1998) 658c
- [8] V.D. Efros, W. Leidemann, and G. Orlandini, Few-Body Syst. **26**, (1999) 251
- [9] S. Martinelli, H. Kamada, G. Orlandini and W. Glöckle, Phys. Rev. **C52**, (1995) 1778
- [10] V.D. Efros, W. Leidemann and G. Orlandini, Phys. Lett. **B408**, (1997) 1;
- [11] V.D. Efros, W. Leidemann and G. Orlandini, Phys. Rev. Lett. **78**, (1997) 432; *ibid* 4015; V.D. Efros, W. Leidemann and G. Orlandini, Phys. Rev. **C58**, (1998) 582
- [12] W. Leidemann, V.D. Efros, G. Orlandini and E.L. Tomusiak, Fizika **B8**, (1999) 135
- [13] C.R. Chen, G.L. Payne, J.L. Friar and B.F. Gibson, Phys. Rev. **C31**, (1985) 2266
- [14] A. Ariaga, V.R. Pandharipande and R.B. Wiringa, Phys. Rev. **C52**, (1995) 2362
- [15] R. De Tourreil, B. Rouben and D. W. L. Sprung, Nucl. Phys. **A242**, (1975) 465 ; J. Côte, R. De Tourreil, B. Rouben and D. W. L. Sprung, Nucl. Phys. **A273**, (1976) 269
- [16] R.A. Malfliet and J. Tjon, Nucl. Phys. **A127**, (1969) 161
- [17] J. O'Connell, Lecture Notes in Physics **260**, (1986) 235
- [18] V. N. Fetisov, A. N. Gorbunov and A. T. Varfolomeev, Nucl. Phys. **A71**, (1965) 305
- [19] D. D. Faul, B. L. Berman, P. Meyer and D. Olson, Phys. Rev. **C24**, (1981) 849, and references therein
- [20] R.B. Wiringa, V.G.J. Stoks and R. Schiavilla, Phys. Rev. **C51**, (1995) 38
- [21] V.G.J. Stoks, R.A.M. Klomp, M.C.M. Rentmeester and J.J. de Swart, Phys. Rev. **C48**, (1993) 792
- [22] V.D. Efros, Sov. J. Nucl. Phys. **41**, (1985) 949
- [23] A. Lapiana and W. Leidemann, paper in preparation

Fig.1

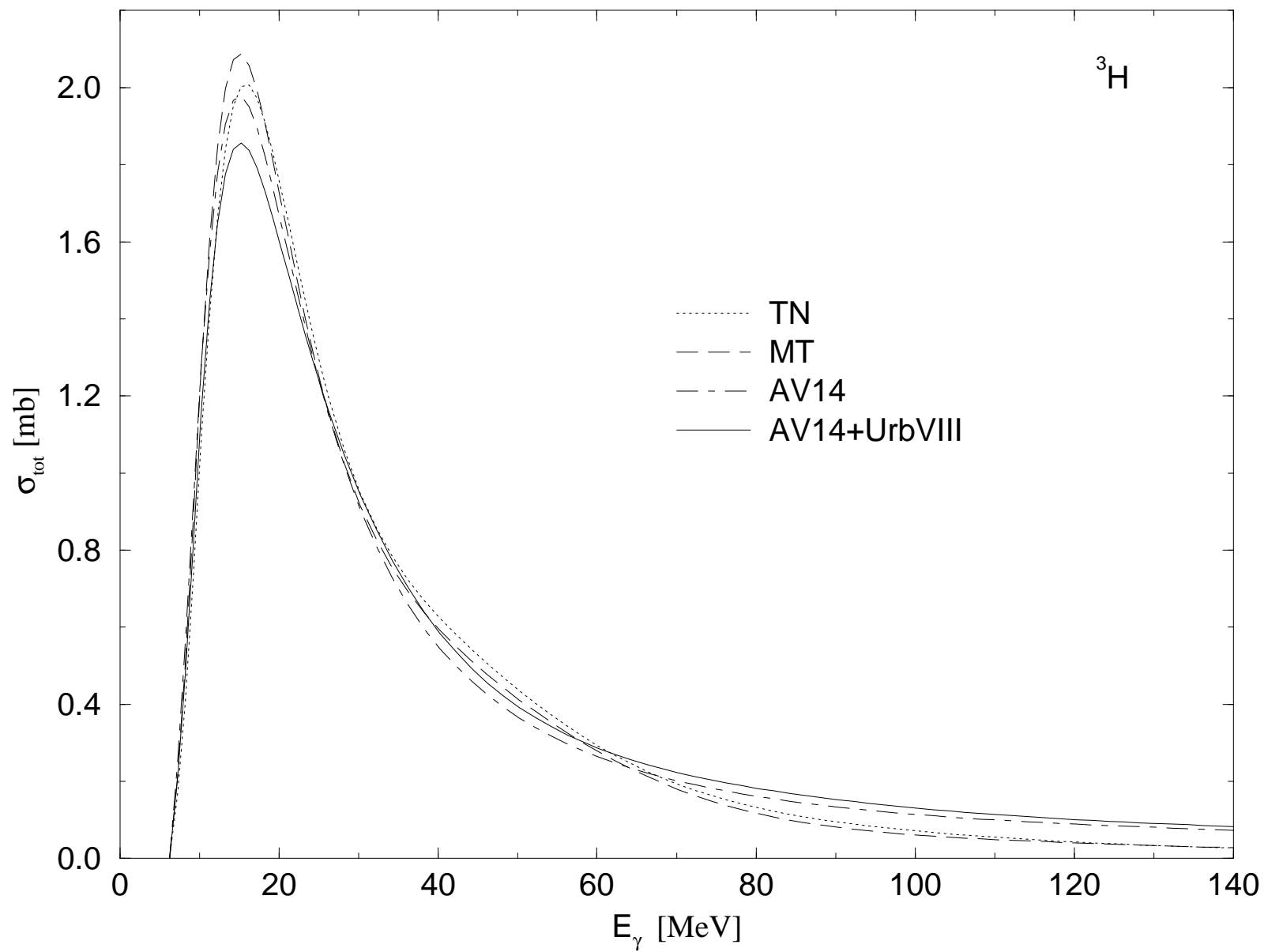


Fig.2

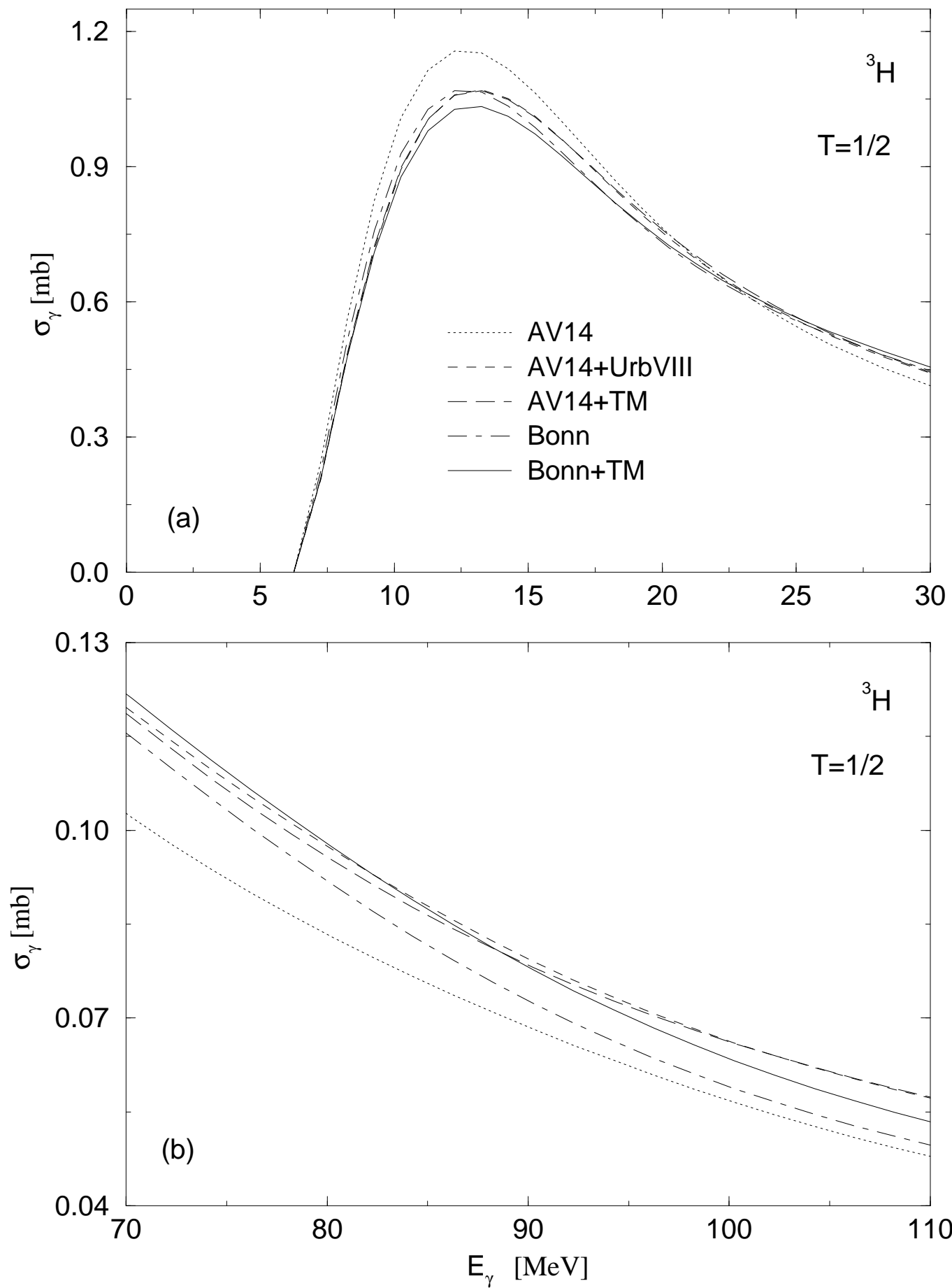
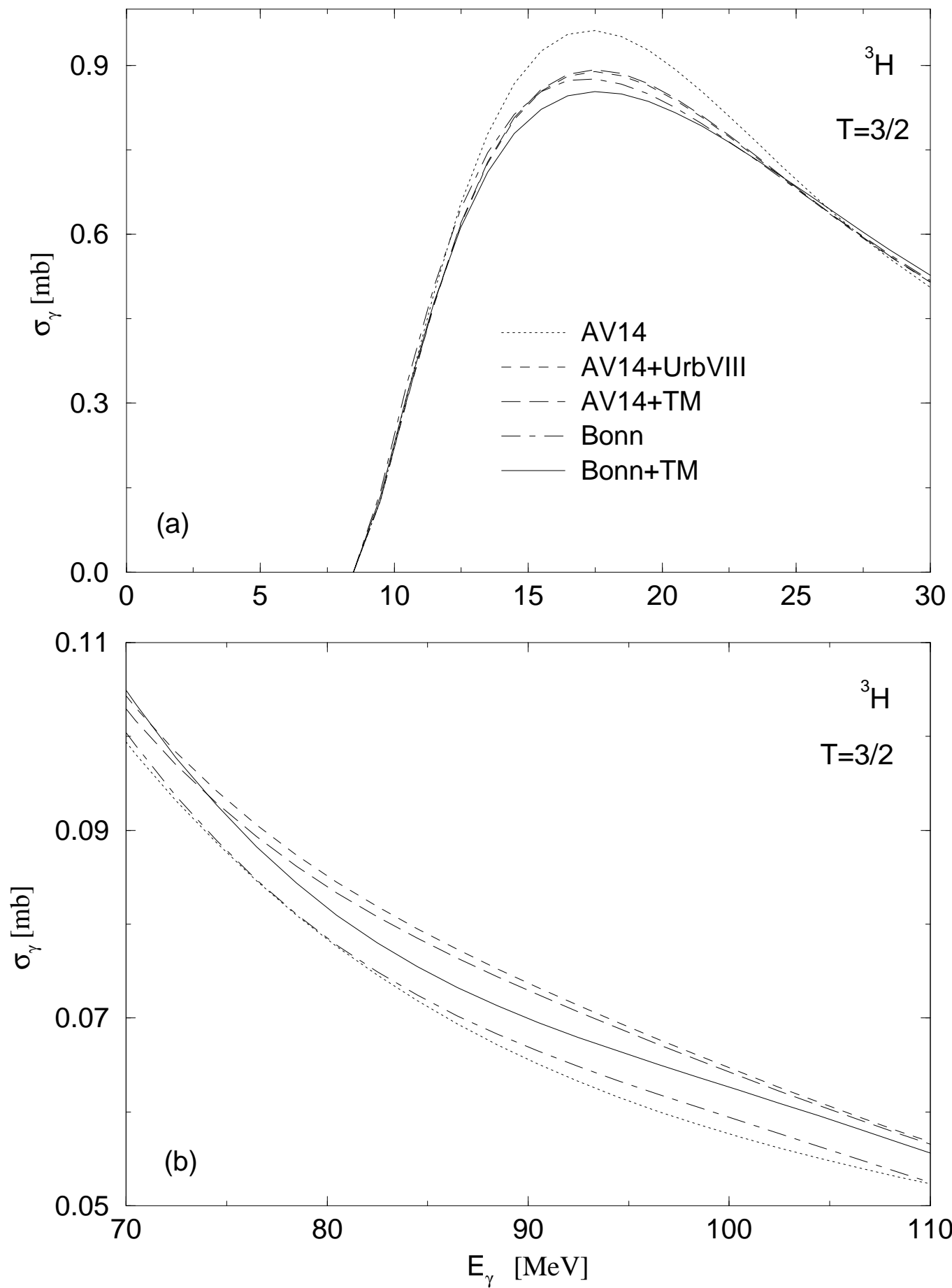


Fig.3



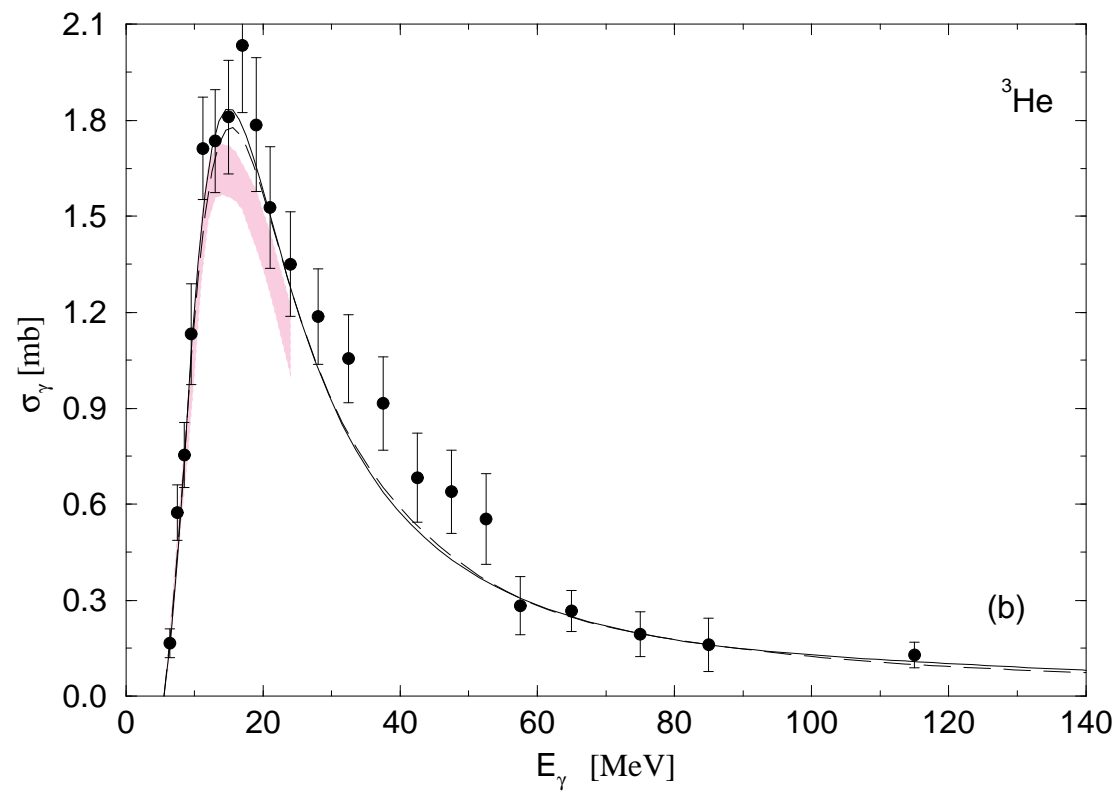
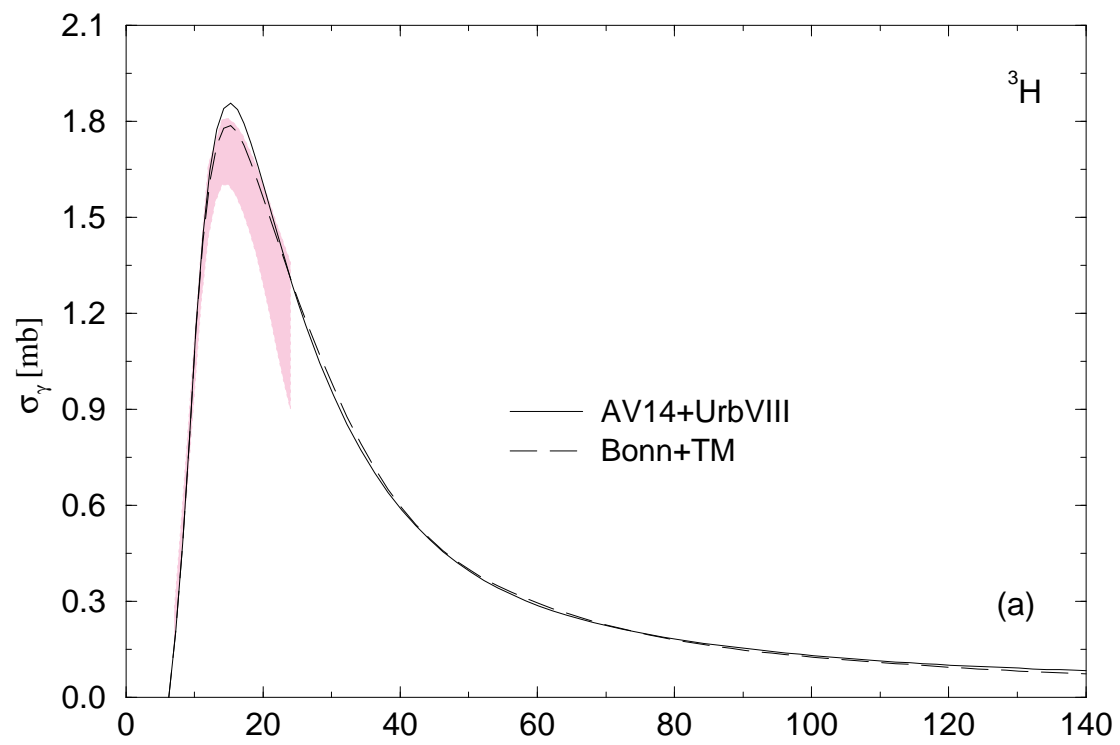


Fig. 4